Recycling of a commercial biodegradable polymer blend: Influence of reprocessing cycles on rheological and thermo-mechanical properties

Irene Bavasso [a,*], Maria Paola Bracciale [a], Giovanni De Bellis [b,c], Alessia Pantaleoni [a], Jacopo Tirillò [a], Genny Pastore [d], Serena Gabrielli [d], Fabrizio Sarasini [a]

[a] Department of Chemical Engineering Materials Environment, Sapienza University of Rome & UdR INSTM, Via Eudossiana 18, 00184, Roma, Italy
[b] Department of Astronautical, Electrical and Energy Engineering, Sapienza University of Rome, Via Eudossiana 18, Rome, 00184, Italy
[c] Research Center on Nanotechnology Applied to Engineering of Sapienza (CNIS), Sapienza University of Rome, Piazzale Aldo Moro 5, Rome, 00185, Italy
[d] ChIP Building, School of Science and Technology, University of Camerino, Via Madonna delle Carceri, 62032, Camerino, Italy

ARTICLE INFO

ABSTRACT

Mechanical recycling is a viable option for reducing plastic waste, especially for post-consumer waste and scraps from production processes. Biodegradable polymers have gained attention as alternatives to conventional ones, and their potential for reprocessing using standard techniques before composting needs to be explored. This study focused on a commercial biodegradable polymer blend which underwent ten extrusion cycles to assess the effects of mechanical recycling on mechanical properties, rheological behavior, and thermal stability. The results indicated that the blend's mechanical properties were largely maintained across the extrusion cycles, with only a 53 % decrease in ductility. The thermal stability slightly declined by 2.3 % in $T_{5\%}$ onset temperature. This can be attributed to a balance between molecular chain scission (resulting in an average molecular weight reduction of approximately 8.4 %) and crosslinking phenomenon (evidenced by an increase in complex viscosity throughout the extrusion cycles). Overall, the results suggest a suitable recycling attitude of this material.

1. Introduction

The significant volume of post-consumer plastics and their environmental consequences throughout their lifecycle underscore the urgency of establishing a sustainable plastic industry. This urgency drives the transition from conventional fossil-based polymers to bio-based and biodegradable alternatives. The increasing interest in these materials stems from their ability to be mineralized over time through biological processes with the production of microbial biomass (biodegradation) and fertilizers (composting) [1]. The microbially induced chain scission process, although capable of degrading bio-based and biodegradable plastics, may not be the most sensible solution for plastic waste minimization due to its sensitivity to various environmental conditions. Factors such as oxygen concentration, humidity, temperature, and pH, as well as the availability and concentration of microorganisms, can significantly influence the degradation rates. Consequently, the degradation process can vary widely and tends to be relatively slow [2]. The necessity of finding alternative solutions for waste disposal, by the waste hierarchy concept outlined in the EU Waste Framework Directive,

extends beyond relying solely on composting as an option [3]. This highlights the importance of exploring recycling strategies that can be implemented through mechanical or chemical techniques. Mechanical recycling is generally cost-effective compared to chemolysis [4], but its implementation requires specific investigations due to the thermo-sensitive nature of biodegradable polymers [5]. Recently Dedieu et al. have summarized their findings on the effect of thermo-mechanical reprocessing (extrusion, injection molding, or compression molding) on the mechanical properties of biopolymers such as polylactic acid (PLA), polyhydroxyalkanoates (PHAs), polybutylene succinate (PBS), and polybutylene adipate terephthalate (PBAT) [6].

Nevertheless, there needs to be more research available, explicitly addressing the effect of reprocessing over biopolymer blends. It is widely recognized that neat biodegradable polymers often require modifications to be competitive with conventional fossil-based polymers in terms of mechanical properties and thermal stability, and melt blending is considered an economical and versatile method to achieve materials with balanced and customized properties [7]. In a study by Zembouai et al. [8], the effect of mechanical recycling on a PHBV/PLA blend

---

* Corresponding author.
E-mail address: irene.bavasso@uniroma1.it (I. Bavasso).

(50/50 wt%) was investigated through six melt molding cycles. The findings of the study indicated that PLA played a stabilizing role in the blend, helping to reduce PHBV degradation during the recycling process. As a result, the tensile modulus, strain at break, and impact strength of the blend remained almost constant throughout the recycling cycles. Farias et al. [9] investigated the properties of a PHBV/PLA blend with a composition of 30/70 wt% for mechanical recycling up to five extrusion cycles. The study demonstrated that the blend maintained good mechanical properties throughout the recycling process, and this was attributed to the reduction of PHBV domains homogeneously distributed within the PLA matrix and the increased crystallinity of PLA. Bourmaud et al. [10] tested a blend of L-Poly-(lactide) (PLLA) and PBS with a 50/50 wt% composition through seven reprocessing (extrusion and injection molding) cycles. The study revealed that the blend exhibited quasi-stable tensile strength and Young's modulus after each recycling operation. However, a significant decrease of 57.3 % of the impact energy at failure was observed after the third cycle. This decrease was attributed to the brittle nature of the blend and the degradation of PLLA, which is susceptible to hydrolysis, which can lead to chain scission and a reduction in molecular weight.

Regarding commercial biodegradable blends, there needs to be more information regarding the effects of reprocessing: Morreale et al. [11] investigated BioFlex F2110, a blend based on PLA and thermoplastic polyesters. They observed that reprocessing minimally affected the blend's quasi-static tensile properties and dynamic thermo-mechanical properties. However, after four recycling cycles, a decrease of 19.5 % in the elongation at break, attributed to the shortening of polymer chains, was noted. Resch-Fauster et al. [12] studied the properties of PHE 001 based on PHBV-PBAT (35/65 wt%). They found that the recyclability of the blend was limited due to significant hydrolysis degradation. The blend exhibited decreased properties with increasing recycling cycles. La Mantia et al. [13] investigated Ecovio (F23B1) reprocessing based on PLA/PBAT. They conducted up to five recycling cycles and observed that the tensile strength of the blend remained relatively constant. However, an increase in Young's modulus and a decrease in the elongation at break were observed due to a reduction in molecular weight and an increase in crystallinity.

Collecting comprehensive information on the reprocessing of biodegradable polymers, particularly on commercial blends, is essential for effectively implementing mechanical recycling at an industrial scale. Commercial blends often consist of proprietary formulations that may not disclose detailed information about their composition or the impact of additives [14] on processing and thermomechanical properties. This makes it challenging to predict the final properties of these blends after recycling.

This study aimed to assess the viability of reusing the scraps from processing a commercial biodegradable polymer blend (Estabio) commonly employed in producing disposable items such as cutlery and coffee capsules. The polymer was subjected to multiple extrusion cycles, up to ten times, to investigate the impact of this recycling process on different properties. The effects were examined in terms of mechanical properties (including tensile strength, flexural strength, Shore D hardness, and Charpy impact tests), thermal stability (analyzed through thermogravimetric analysis, differential scanning calorimetry, and dynamic mechanical analysis), rheological properties and morphology (observed via scanning electron microscopy).

2. Materials and methods

2.1. Materials and sample preparation

Commercial polyester Estabio (PL 0640 T05) was purchased from Fi-Plast S.r.l. The material was dried at 60 °C overnight before the reprocessing operation through extrusion (corotating twin-screw extruder, Thermo Scientific Process 11, ThermoFisher Scientific) and injection molding (Haake MiniJet II Pro, Thermo Fisher Scientific) with

the adoption of a temperature profile as follows: 170 °C—175 °C—180 °C—185 °C—190 °C—195 °C—195 °C–195 °C (from zone 1 to 8, respectively). The rotational speed was set at 150 rpm. During the injection, the mold and the loading cylinder were maintained at 45 °C and 190 °C, respectively. To simulate the multiple melt processing, after each injection, the polymer was pelletized for the following cycles up to a maximum number of extrusions and injections equal to ten. The samples were named "Ext n," where n is the number of extrusion/injection cycles.

2.2. Composites characterization

2.2.1. FTIR spectroscopy

Molecular characterization was performed by Fourier Transform InfraRed (FT-IR) spectroscopy. IR spectra were acquired on a Bruker VERTEX 70 spectrometer, equipped with a diamond attenuated total reflectance (ATR) cell, in the mid-infrared region (400 - 4000 cm^{-1}) and collecting 256 scans with a resolution of 3 cm^{-1}.

2.2.2. Thermal properties

Thermogravimetric (TGA) analysis was carried out by heating the samples from room temperature to 800 °C under a nitrogen atmosphere and with a heating rate of 10 °C/min (Setsys Evolution system by Setaram).

Differential scanning calorimetry (DSC) analysis of the materials was performed under a nitrogen flow of 60 mL/min (DSC 214 Polyma by Netzsch). Specimens (around 10 mg) were placed in a concave crucible with a pierced lid and analyzed according to the following thermal program: heating from −40 °C to 200 °C (5 min hold interval), cooling to −40 °C (5 min hold) and second heating to 200 °C, all steps performed with a rate of 10 °C/min. Results as melting and crystallization temperatures and enthalpies are reported as mean values of three repetitions.

Dynamic mechanical analysis (DMA) in a three-point bending configuration was used to measure the properties of the manufactured samples (with size 60 × 10 × 4 mm) under dynamic conditions from −160 °C to 60 °C, with a heating rate of 2 °C/min and a frequency of 1 Hz. The tests were conducted by using a DMA 242 E Artemis by Netzsch and the storage (E′) and loss moduli (E″), and the loss (damping) factor tanδ (E"/E') were measured.

2.2.3. Rheological properties

Rheological properties were investigated through an Anton Paar MCR302 rotational Rheometer (Anton Paar - Graz, Austria) equipped with a 25 mm plate-plate measuring system. Dynamic measurements were carried out at 190 °C under a nitrogen flow of 230 L/h. The linear-viscoelastic region (LVR) limits were investigated by running amplitude sweeps in the shear strain range between 0.1 and 100 % at a constant angular frequency of 1 rad/s. A shear strain of 0.1 %, falling within the LVR, was then chosen to run the following frequency sweeps in the range of angular frequencies between 0.1 and 100 rad/s. Specimens for rheological measurements were obtained by laser cutting (Birio 1000, 100 W CO$_2$ laser) 25 mm diameter discs from compression molded plates (at 190 °C), with thickness around 1 mm. All the tests were repeated on three samples, and the results are reported as mean values.

The melt flow rate of each processed biopolymer was measured using a plastometer (Zwick/Roell Mflow) at 190 °C with a 2.16 kg nominal load adapted to the standard ISO 1133. The results are reported in terms of melt mass flow rate (MFR) as a mean value of three repetitions.

2.2.4. Mechanical properties

The tensile and flexural tests of all manufactured specimens were carried out on a Zwick/Roell Z010 universal testing machine. Tensile tests were conducted in displacement control with a 10 mm/min crosshead speed at room temperature according to ISO 527-2 (type 1BA, L_0 = 30 mm). Three-point bending tests determined flexural properties

of the materials according to ISO 178. Samples (with size 80 × 10 × 4 mm) were tested at 5 mm/min with a span-to-thickness ratio of 16:1. The impact strength of each sample (with size 80 × 10 × 4 mm) was evaluated by Charpy impact tests (ISO 179-2) in an edgewise mode (type A notch and a span of 62 mm). Tests were conducted with a CEAST/Instron 9340 instrumented drop weight tower using an impact velocity of 2.90 m/s and at three different temperatures (25 °C, 50 °C and 80 °C). All tests were repeated at least five times and reported as mean values.

The hardness of the extruded biopolymers was measured using an analog hardness shore D tester (Zwick/Roell GmbH, Ulm, Germany) according to ASTM D-2240. The hardness value for each sample was calculated as the average of 50 measurements at room temperature.

2.2.5. Morphological properties

Fracture surface morphologies of biopolymers were studied using scanning electron microscopy (FE-SEM Mira3 by Tescan) equipped with an Octane Elect EDS System by EDAX (AMETEK GmbH, Unterschleissheim, Germany). All specimens were sputter-coated with gold before the analysis.

2.2.6. Nuclear magnetic resonance (NMR)

The ^{1}H NMR spectra were recorded by Varian Mercury 400 (400 MHz). The chemical shifts δ are in ppm and are referenced to residual protons in the deuterated solvent as the internal standard, such as CDCl3 (7.26 ppm). Splitting patterns are s, for singlet; d, for doublet; t, for triplet; q, for quartet, and m, for multiplet.

2.2.7. Gel permeation chromatography (GPC)

The measurements of molecular weights were performed by Agilent 1260 Infinity II Multi-Detector Suite (MDS) device, constituted by three different detectors (G7800A): RI, VS and dual light scattering detector (15° and 90°), a 4-channel vacuum degasser (G7111B), an autosampler (G7129A) and a thermostatic column compartment (G7116A). The system was equipped with a guard column (Agilent GPC/SEC Guard Column), followed by two columns in series (PLgel MIXED-C and PLgel MIXED-D) and the measurements were processed by Agilent GPC/SEC Software. The THF mobile phase contained 250 ppm of BHT (butylated hydroxytoluene), and the flow rate was fixed at 1.0 ml/min. The polystyrene standards (Mp values in the range of 580–283800 g/mol) were used for column calibration.

3. Results and discussion

3.1. As-received polymer blend characterization

This section provides an overview of the properties of neat Estabio, focusing on its chemical properties and thermal stability. While the exact chemical composition of the product is undisclosed due to patent protection, the major components of the material were identified using FT-IR and EDS mapping (Fig. 1) and ^{1}H NMR (Fig. 2) analyses.

The infrared spectrum reported in Fig. 1a displays distinctive bands indicating the presence of Poly(butylene succinate) (PBS) at 1714, 1157, 955 and 806 cm^{-1}, arising from the stretching vibrations of ester carbonyl (>C=O) group, –C–O–C– group in the ester linkages and from bending of –C–OH groups in carboxylic acid, respectively [15]. Additionally, the absorptions at 1330, 2946, and 2850 cm^{-1} are linked to the stretching vibrations of methyl and methylene C–H groups in the PBS main chain [15]. Weaker signals associated with polylactic acid (PLA) were identified at approximately 1756 cm^{-1} (stretching of the C=O carbonyl group), 1449 cm^{-1} (bending of –CH$_3$ groups) and 1386, 1357
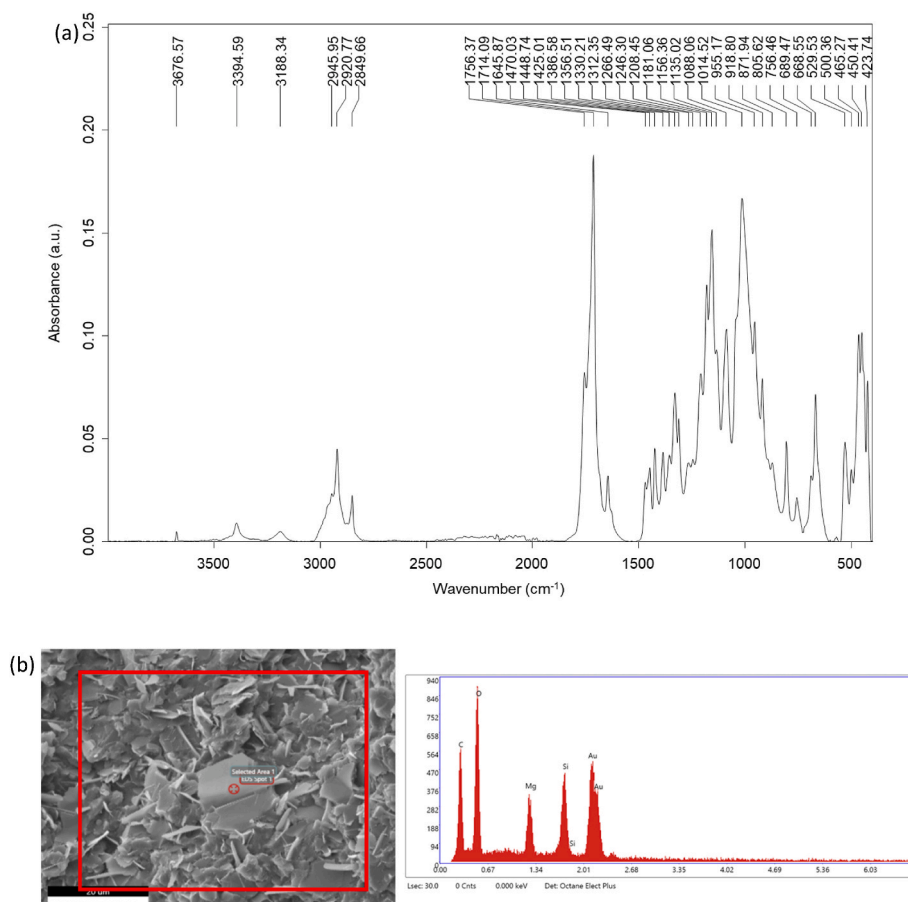

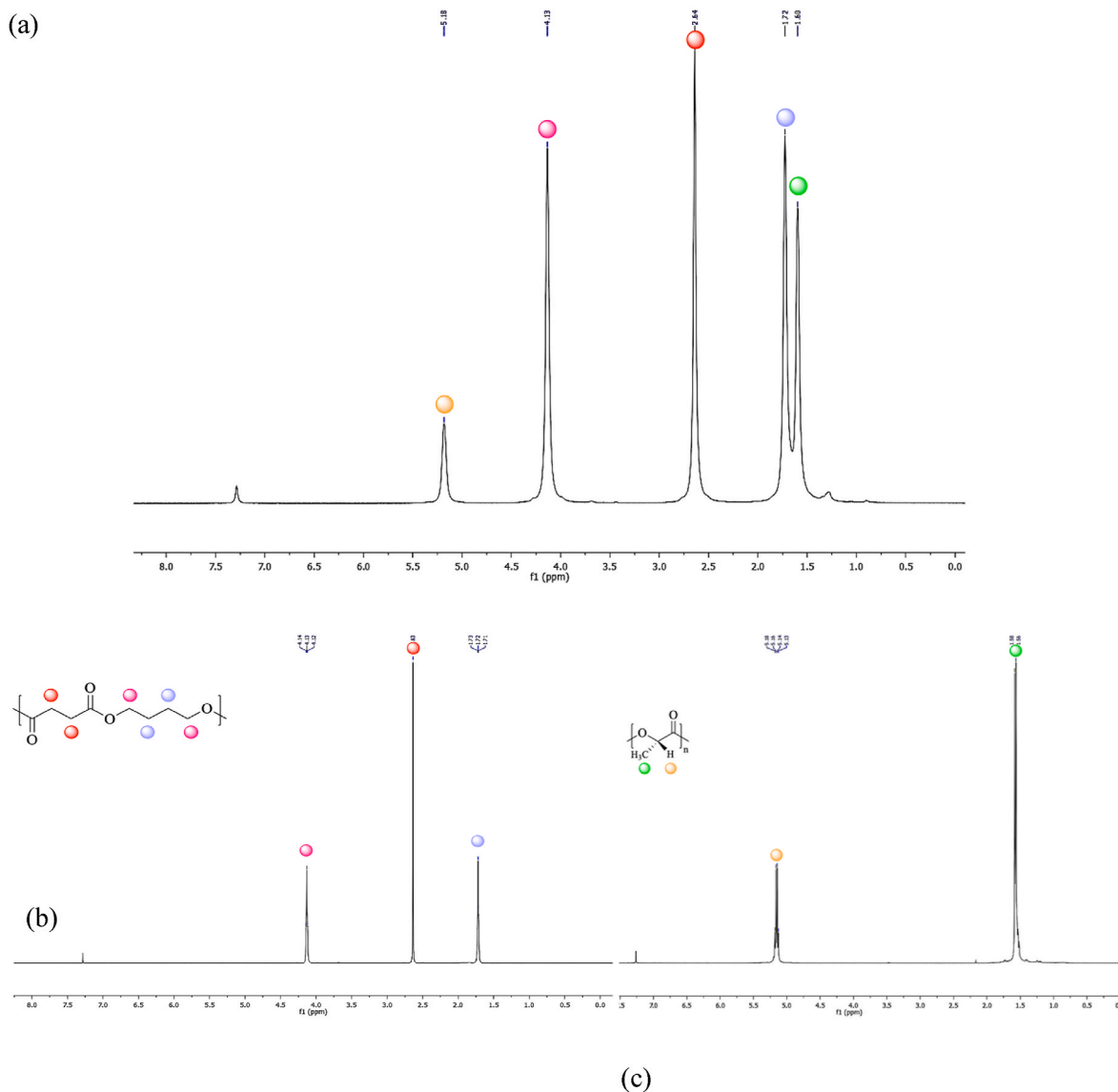**Fig. 1.** Infrared spectrum (a) and EDS mapping (b) of neat polymer.

(a)

(b)

(c)

Fig. 2. ^{1}H NMR spectra of (a) neat polymer, (b) PBS and (c) PLA.

cm^{-1} (deformation of -C-H bonds). Further absorptions at 1181, 1135, and 1088 cm^{-1} originated from the stretching vibrations of -C-O groups within PLA [16]. Vibration bands due to magnesium silicate [Mg$_3$Si$_4$O$_{10}$(OH)$_2$] at 3677, 1015, and 669 cm^{-1}, and stearamide [C$_{38}$H$_{76}$N$_2$O$_2$] at 3395, 3188, 1646, 1470, and 1425 cm^{-1}, were also detected [17,18]. These additives are used to improve the strengthening,
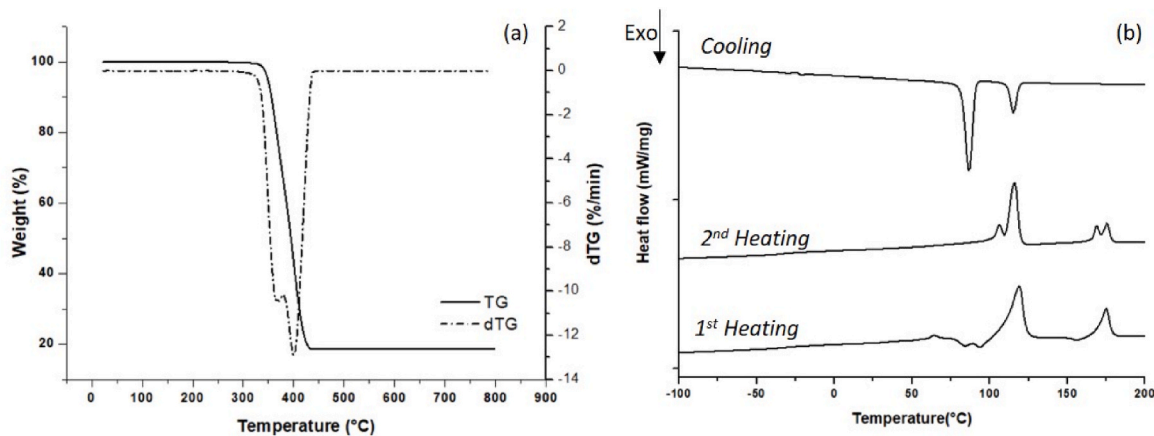

Fig. 3. (a) TG and dTG curves and (b) DSC thermograms of neat polymer.

lubricating properties, and mobility and nucleation capacity of PLA.

This evidence is corroborated by ^{1}H NMR results of Estabio (Fig. 2a) that were compared with those of neat PLA and PBS (Fig. 2b–c). The peaks observed at 1.72 ppm (-OCH_2*CH_2CH_2*CH_2O-), 2.64 ppm (-O=C*CH_2CH_2*C=O-), and 4.13 ppm (-O*CH_2*CH_2CH_2*CH_2*O-) in the spectrum can be attributed to the distinct methylene proton signals of PBS [19,20], further supported by the results obtained from the standard PBS sample in Fig. 2b. Additionally, peaks at 1.60 ppm and 5.18 ppm correspond to the CH_3- and CH- proton signals, respectively [21], which are also consistent with the ^{1}H NMR spectrum of neat PLA.

The blend exhibited a thermal degradation with two close peaks, one at 361 °C and a second one at 398 °C with associated weight losses equal to 21.4 wt% $\pm$ 0.8 wt% and 58.0 wt% $\pm$ 0.1 wt%, respectively (Fig. 3a). This two-stage thermal degradation process provides further confirmation of the prevalence of two polymers in the blend with a certain level of immiscibility between them [9,22], and according to both thermal degradation temperatures measured, it is possible to associate the first peak to PLA [9] and the second one to PBS [23]. The mass residue at 800 °C equal to 18.1 % is ascribed to the presence of talc [$Mg_3Si_4O_{10}(OH)_2$] (Fig. 1a–b), which is commonly used as a nucleating agent and/or reinforcing filler in biopolymer blends [24–27].

From DSC results (Fig. 3b), during the first heating and cooling cycle it is possible to identify the glass transition (T_g) at 60 °C, the melting (T_m) and the crystallization (T_c) peaks at 175 °C and 115 °C, respectively, typical values of PLA [28]. Meanwhile, temperatures equal to -28 °C, 115 °C, and 86 °C are those of glass transition, melting, and crystallization points of PBS [29]. In addition, the cold crystallization of PBS (at around 84 °C [30]) and of PLA (at 93 °C [31]) were detected. The controlled cooling impacts the second heating cycle, leading to the absence of cold crystallization peaks and the appearance of a dual-shaped melting peak for both polymers. The former is attributed to the formation of thinner crystals, while the latter is associated with the development of thicker ones [31,32]. As the polymer blend's exact composition is unknown, an estimation of the crystallinity of both polymers was determined by considering the weight losses from the thermogravimetric curves. The degree of crystallinity for PLA was calculated to be approximately 60.19 % $\pm$ 0.85 %. In comparison, for PBS it was found to be about 74.7 % $\pm$ 2.8 % (the adopted ΔH_m^0 as the standard enthalpy of melting of 100 % crystalline PBS and PLA was equal to 200 J/g and 93 J/g, respectively [33]).

3.2. Thermal properties of recycled polymer blends

To assess the recyclability of the commercial blend, ten recycling operations were simulated using repeated extrusion and injection molding cycles. The thermogravimetric analyses were conducted after each extrusion/injection cycle, and the results of the most representative samples (Ext 2, Ext 5 and Ext 10) as weight loss and derivative thermogravimetry (dTG) trend are reported in Fig. 4 a-b. The recycling process led to a slight reduction in the thermal stability of the blend. The initial onset temperature value (corresponding to a weight loss of approximately 5 %) of the pristine Estabio was 348.7 °C, which decreased by around 2.3 % after the last extrusion/injection cycle adopted in this work (Ext 10).

Specifically, the calculated onset temperature values were 347.0 °C (Ext 1), 344.4 °C (Ext 2), 344.1 °C (Ext 3), 343.7 °C (Ext 5), 342.1 °C (Ext 8), and 340.5 °C (Ext 10). This effect can be attributed to PLA, as its thermal degradation temperature decreased from 367 °C to 357 °C (Fig. 4b inset). The observed decrease in PLA's thermal stability had a minimal impact on the overall stability of the blend, mainly because PLA is present in a smaller proportion compared to PBS.

A weight loss of approximately 10 % for neat Estabio was obtained at a temperature of 355.8 °C. Such weight loss after each recycling cycle was recorded at 355.0 °C (Ext 1), 351.4 °C (Ext 2), 351.5 °C (Ext 3), 351.4 °C (Ext 5), 350.7 °C (Ext 8), and 350.1 °C (Ext 10) and the reduction in thermal stability of the blend after the tenth extrusion/
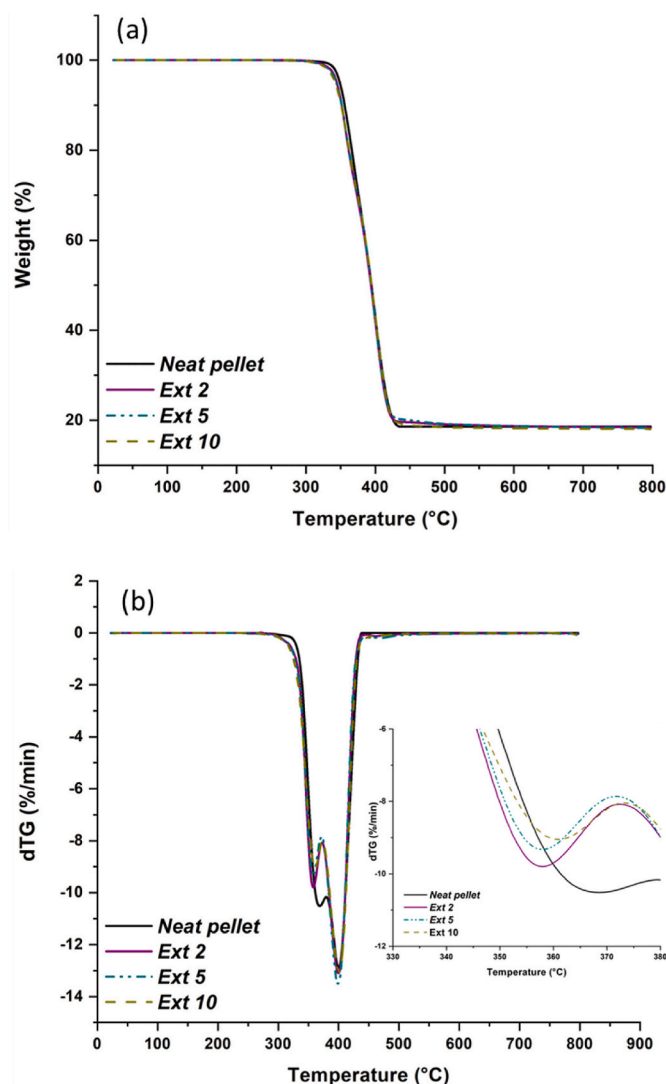

Fig. 4. (a) TG and (b) dTG curves of reprocessed polymer blend.

injection cycle was around 1.6 %. As the temperature rises, the difference in degradation profiles becomes less pronounced, highlighting how, unlike PLA, PBS seems to be less affected by reprocessing. This finding aligns with the results reported by Ojijo et al. [34], indicating that a PBS-dominated blend exhibits higher thermal stability. Furthermore, this slight effect on thermal stability can be attributed to the fact that the initial decomposition temperature of the blend was significantly higher than the processing temperature employed in the recycling process.

An estimation of the PLA and PBS amounts was derived by analyzing the thermogravimetric trends (Fig. 4a) at the thermal degradation temperatures of each polymer. The PLA content decreased from 21.0 % (Ext 1) to 14.1 % (Ext 10), while the PBS content showed a slight decrease from 58.0 % (Ext 1) to 55.7 % (Ext 10).

The calorimetric results, consistent with the thermogravimetric analysis findings, did not show significant differences in the thermogram trends (Figs. S1a–b). The temperatures and enthalpy values for the cooling and second heating cycles are provided in Table 1.

The reprocessing operation did not significantly alter the characteristic temperatures of both polymers. However, the most notable effect of the processing was observed in the variation of the melting enthalpy of both polymers calculated as the difference of enthalpy measured after each reprocessing cycle and the melting enthalpy calculated after the first extrusion. Fig. S1c demonstrates that reprocessing led to a

Table 1
DSC results.

Sample	2nd Heating cycle								Cooling			
	PBS				PLA				PBS		PLA	
	T_{m1} (°C)	ΔH_{m1} (J/g)	T_{m2} (°C)	ΔH_{m2} (J/g)	T_{m3} (°C)	ΔH_{m3} (J/g)	T_{m4} (°C)	ΔH_{m4} (J/g)	T_{c1} (°C)	ΔH_{c1} (J/g)	T_{c2} (°C)	ΔH_{c2} (J/g)
Ext 1	105.2	5.81	115.0	28.36	168.4	2.29	175.2	3.74	86.9	34.37	116.0	10.92
Ext 2	105.2	5.16	115.7	28.96	168.7	2.50	175.5	3.48	85.9	37.27	115.8	11.50
Ext 3	105.4	5.40	115.0	28.65	168.5	2.33	175.3	3.62	86.8	37.29	115.9	10.98
Ext 5	105.1	5.43	115.2	28.59	168.5	1.96	175.2	3.79	86.4	36.83	116.1	10.85
Ext 8	105.3	3.57	116.1	27.53	168.9	1.69	175.5	2.98	85.3	34.42	115.6	10.47
Ext 10	105.1	3.12	116.0	27.35	168.8	1.65	175.4	2.90	85.1	34.90	115.7	10.92

significant reduction in the melting enthalpy of PLA. This decrease in enthalpy is believed to be connected to a more substantial reduction in crystallinity for PLA compared to PBS. Specifically, the reduction in crystallinity was approximately 20 % for PLA and 11 % for PBS.

To confirm such evidence, FT-IR spectra of neat and post-processed polymers (Ext 1, Ext 2, Ext 5 and Ext 10) are reported in Fig. 5.

The poor heat resistance of PLA, previously detected, was confirmed by observing a decrease in the intensity of the band at 1756 cm^{-1} in the extruded polymers. Indeed, by the integrated area ratio of the absorptions at 1756 cm^{-1} (C=O carbonyl group of PLA) and 1713 cm^{-1} (>C=O of PBS) [15,16], it has been noted that the amount of the PLA decreased from 21 % to 13 % after the 10th cycle (values in agreement with thermogravimetric results). The bands at 1209 and 920 cm^{-1} are generally associated with the absorptions of a highly crystalline polymer [35,36]. Furthermore, the band centered at 919 cm^{-1} is correlated to the α and α′ crystalline forms, and the band at 955 cm^{-1} is assigned to the amorphous phase [36] Fig. 5 also highlights a noticeable reduction in the intensity of the bands at 1209 and 1181 cm^{-1} as the reprocessing cycles increase, which is correlated with the amorphization of PLA samples. Indeed, the crystallinity indexes, calculated as the ratio between band intensities at 1209/1181 [37,38], were initially higher for the pure blend (approximately 65 %) but decreased to 53 % after the 10th reprocessing cycle. These findings confirm the DSC results.

3.3. Rheological properties

With the aim of investigating the effect of reprocessing cycles on rheological properties, the results of frequency sweeps on polymer blends Ext 2, Ext 5 and Ext 10 are reported in Fig. 6 in terms of complex viscosity (μ^*, Fig. 6a), storage (G′, Fig. 6b) and loss (G″, Fig. 6c) moduli over the investigated angular frequency range.

Regardless of the number of extrusions, all investigated materials displayed a decreasing value of the complex viscosity (Fig. 6a) with

Fig. 5. FT-IR results of neat and reprocessed polymers.

increasing angular frequencies, indicating a strong shear thinning tendency. Such values are in the range of those of PLA/PBS blends with a typical non-Newtonian behavior [39] and with the disappearance of the inflection point indicating the absence of relaxation phenomena [40]. In Fig. 6b–c, it is evident that the complex viscosity experiences a slight increase with extrusion cycles. This is a result of the simultaneous enhancement of both storage and loss moduli as reprocessing proceeds. Particularly at low frequencies, the reduction in the slope of G′ (Fig. 6b), for increasing number of reprocessing cycles, indicates a clear enhancement in the elastic behavior [41]. In contrast, the impact of reprocessing on rheological properties is less pronounced at higher frequencies.

Jin and colleagues noticed a similar trend during the recycling of low-density polyethylene and attributed the finding to competitive and simultaneous chain scission and crosslinking reactions [42]. A similar trend was observed by La Mantia et al. [13] during the thermo-mechanical recycling of the Ecovio polymer, claiming that this impact is connected to the creation of crosslinks or branching. In this work, it is reasonable to hypothesize the presence of crosslinking or branching phenomena specifically for the PBS component [43]. On the other hand, for PLA, as indicated by the previous results (TG, DSC and FT-IR), its limited thermo-mechanical stability is predominantly linked to degradation processes, such as hydrolytic or radical mechanisms [44], mostly leading primarily to chain scission.

During frequency sweep tests, at 190 °C and 0.1 % shear strain, for increasing recycling cycles a larger increase in the elastic response over the viscous one (G′>G″) was observed, especially for the high frequency region, with a delayed transition to a viscous character (Fig. 7a). Such a difference was not seen during the amplitude sweep at 190 °C and 1 rad/s angular frequency, where the yield point was achieved with a similar trend and with a strain close to 6.9 % ± 2.1 % (Fig. 7b).

Even though rheological evidence suggests that PBS crosslinking between polymer molecules occurs, the mechanical shear forces and thermal effects involved in the extrusion/injection processes [8,45] also resulted in a PLA molecule chain scission event, as proven by changes in weight average molecular weight (M_w), number average molecular weight (M_n) and polydispersity index (PDI as M_w/M_n) summarized in Table S1, and melt-mass flow rate (MFR) values plotted in Fig. 8.

In general, when comparing the melt flow rate (MFR) value of the neat pellet with that of the first extrusion (Ext 1), there is a noticeable increase of approximately 43 %. Moving from Ext 1 to Ext 10, additional increases in this parameter were observed after the fifth and tenth extrusion cycles. Specifically, there was a 3.7 % increase in MFR at Ext 5 and a significant 40.5 % increase at Ext 10. These increments are primarily attributed to the random scission of molecules during the recycling process, as indicated by the trends in the polydispersity index (PDI) outlined in Table S1 [46,47]. Moreover, the presence of just one curve from GPC measurements could be explained by the presence of two phases with similar molecular weights, so they are subtended to the same chromatographic curve. The scission primarily affected the PLA component of Estabio, leading to a reduction in thermal stability (as depicted in Fig. 4) and a significant increase in the flowability of the melted polymer after multiple recycling cycles, specifically after at least
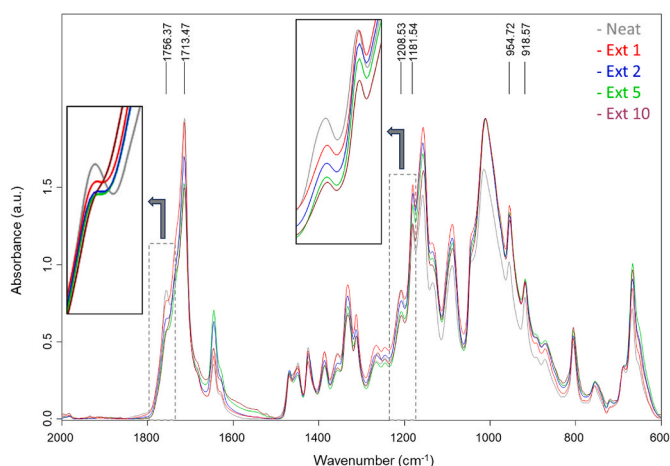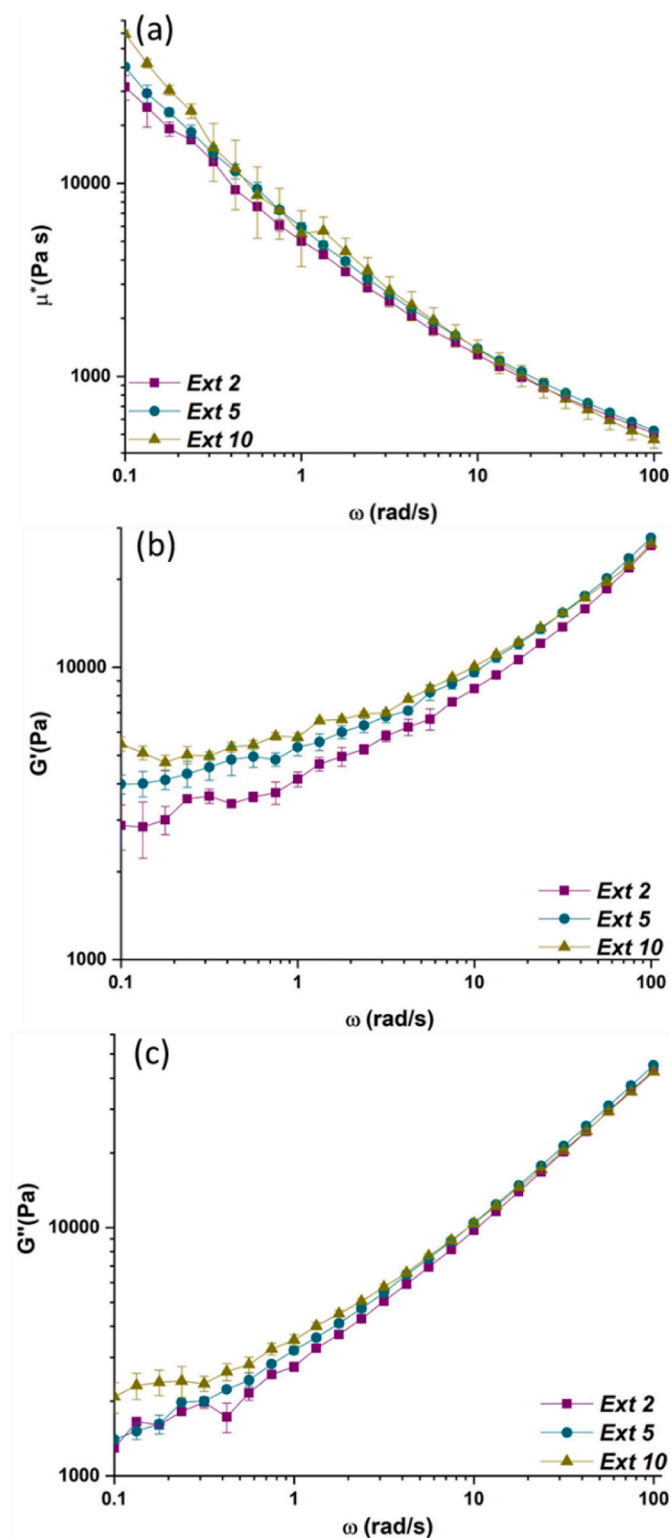
Fig. 6. Frequency sweep results.

five cycles. The high thermal sensitivity of PLA has been demonstrated in various studies. It is well-known that PLA is prone to undergo thermal degradation and exhibits a reduced thermal stability under certain conditions (temperature, shear rate, oxygen) [48]. For instance, Bour-maud et al. demonstrated the extreme thermal sensitivity of PLLA in their study [10]. They observed that PLLA experienced significant degradation after the fourth recycling cycle over PLLA/PBS (50/50 wt %) blends. Additionally, Srimalanon [49] confirmed the prevalence of

chain scission phenomena through additional reprocessing of a PLA/PBS blend (80/20 wt%) for three cycles. The notable increase observed after the initial extrusion cycle (Ext 1) is probably the result of the simulta-neous occurrence of chain scission and the improved distribution and promotion of chain mobility action of the stearamide during the extru-sion process [50–53].

Such evidence is also visible in the DMA results reported in Fig. 9 as storage modulus (E', Fig. 9a) and dynamic damping factor (Tanδ, Fig. 9b). The curves do not reveal any substantial differences regarding the storage moduli as evidenced by the recorded E′ values across the temperature range between −100 °C and 90 °C (Table 2) and this is consistent with results previously discussed, as well as with other works [8,12].

The most significant decrease in E′ was observed near the first glass transition temperature at around −20 °C, as confirmed by the Tanδ trends (Fig. 9b) and ascribed to PBS polymer, because of the softening of the major component in blend formulation. From Tanδ an additional peak (around 62 °C) is visible while approaching PLA's glass transition. At this point, a slight increase in Tanδ value of about 6.9 % (inset in Fig. 9b) indicates a more viscous attitude of PLA due to the occurrence of short molecule motion [54,55]. As a general comment, the trends of both E′ and Tanδ remained similar throughout the multiple reprocessing cycles, indicating the good recyclability of the blend.

3.4. Mechanical properties

The stress vs. strain curves of the reprocessed polymers are reported in Fig. 10, where results were obtained through tensile (Fig. 10a) and three-point bending (Fig. 10b) tests under quasi-static conditions. As regards tensile tests, the simultaneous occurrence of both cross-linking and chain scission, as discussed earlier, has notable effects on the me-chanical properties, as indicated in Table 3. The reduction in elongation at break throughout the reprocessing cycle, as shown in the inset of Fig. 10a, becomes particularly significant after the third extrusion cycle, leading to a substantial decrease in ductility by approximately 22.0 %. This observed reduction in ductility is attributed to two main factors: i) the occurrence of PLA hydrolysis phenomena and chain scission [10,49], supported by the DMA results displaying the shift of PLA T_g in Fig. 9b–and ii) the cross-linking, which not only decreases molecular mobility but also contributes to an increase in the stiffness of the reprocessed material [56] and serves to counterbalance the decrease in polymers crystallinity. Despite the degradation of PLA, the reduction in tensile strength was relatively smaller, primarily influenced by the properties of PBS, because its higher proportion in the blend [57].

From the three-point bending tests (Fig. 10b), the mechanical property losses were only noticeable after the eighth cycle, resulting in a reduction of approximately 6.4 % in flexural strength. However, the flexural modulus remained relatively constant throughout the reproc-essing cycles (Table 3) and hardness resulted in a substantial constant value from 69.3 ± 1.7 (Ext 1) to 73.9 ± 2.6 (Ext 10).

The impact strength of the blends at different numbers of reproc-essing cycles is presented in Fig. 11. The impact tests were conducted at three different temperatures (up to 80 °C), and the specimens exhibited similar impact strength values, indicating no significant effect of the multiple reprocessing cycles up to 50 °C. However, at 80 °C, the notched impact energy decreased from the third extrusion cycle to the fifth cycle by 21.3 %, and by the tenth cycle, it decreased by 39.5 %. The decrease in ductility is consistent with the findings and insights drawn from quasi-static results, particularly noticeable at the highest temperature due to the blend's softening and its proximity to the melting temperature of PBS. At both 25 °C and 50 °C, the materials exhibited a brittle fracture behavior, while at 80 °C, a ductile fracture was observed, evident from the notable plastic deformation (Fig. 12 c-d). Analyzing the micro-graphs, from Ext 1 (Fig. 12 a-c) to Ext 10 (Fig. 12 b-d), no significant impact of mechanical reprocessing on blend characteristics was apparent. The images displayed a continuous polymer phase and
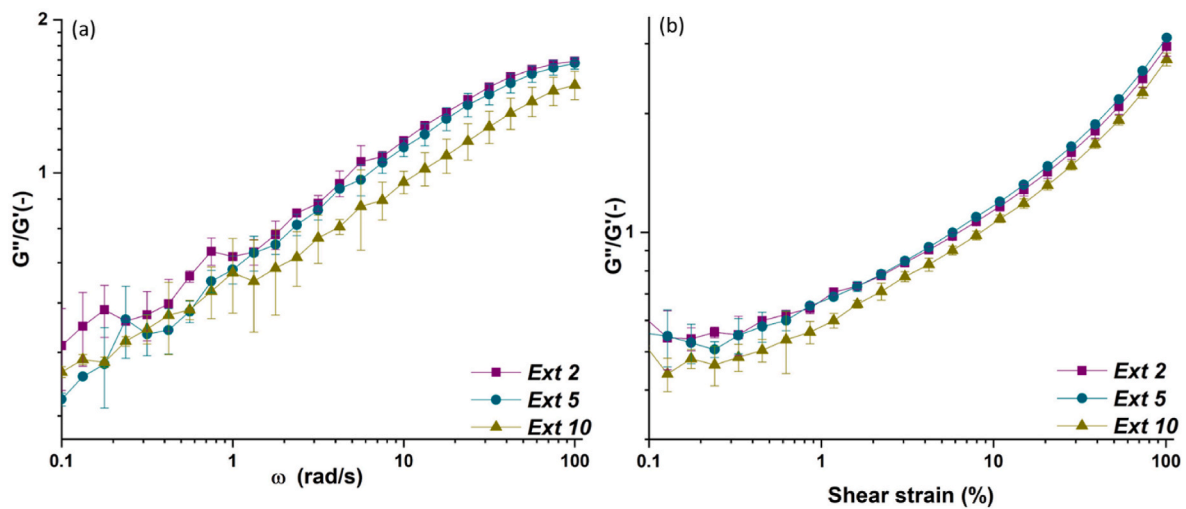
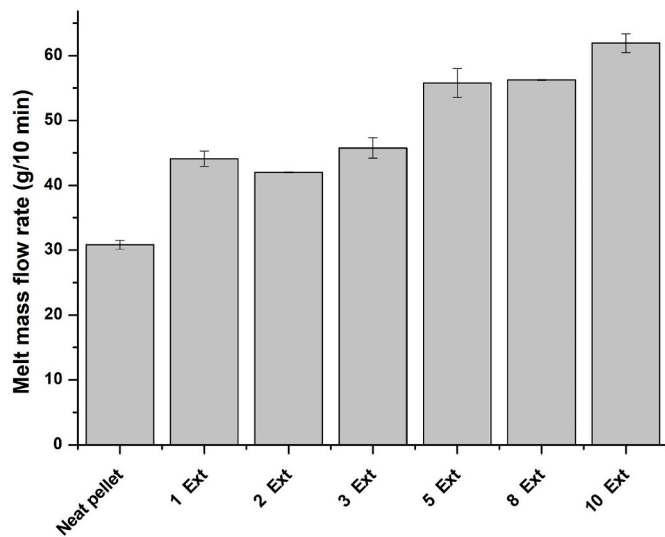**Fig. 7.** Loss factor trends during (a) frequency and (b) amplitude sweep tests.

Fig. 8. Melt Mass Flow rate results.

dispersed plate-like inorganic filler. However, from Ext 1 to Ext 10 at 25 °C, the surface appeared slightly softened, probably ascribed to PLA chain scission and reduced crystallinity occurring during the mechanical reprocessing.

4. Conclusions

The aim of this study was to explore the recycling potential of a commercial biodegradable PLA/PBS polymer blend through multiple reprocessing cycles, up to ten, via extrusion and injection molding. The investigation focused on analyzing the mechanical properties, rheological behavior, and thermal stability of the recycled material. During the

Table 2
Storage Modulus (E') values at different temperatures of reprocessed polymers.

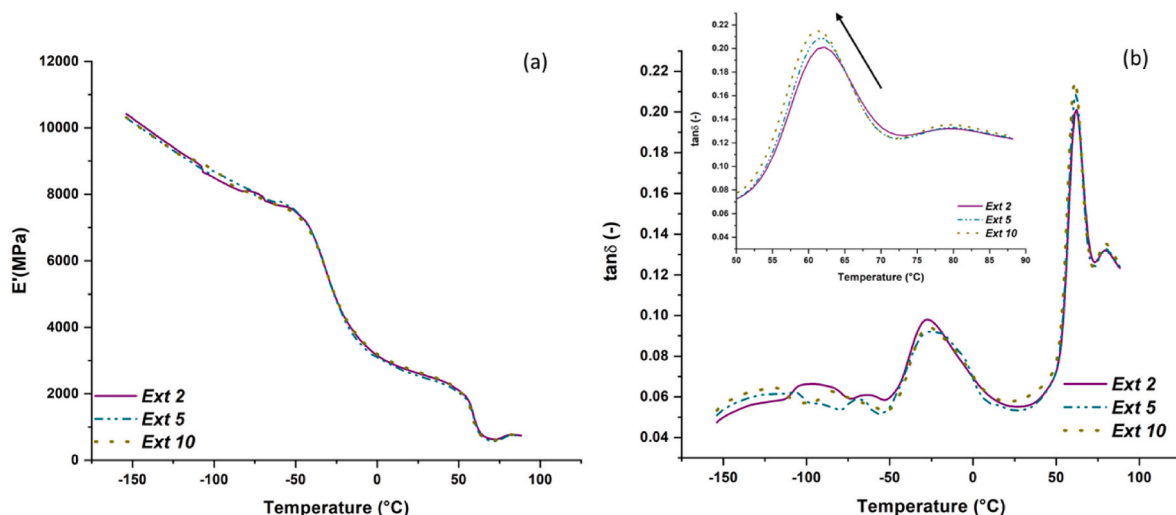| Sample	E' (MPa) at −100 °C	E' (MPa) at 0 °C	E' (MPa) at 25 °C	E' (MPa) at 50 °C
Ext 1	8851.16	3220.72	2553.26	1955.98
Ext 2	9310.48	3369.72	2618.22	2001.37
Ext 3	8761.46	3199.53	2477.61	1931.16
Ext 5	9190.46	3401.58	2642.05	2048.59
Ext 8	8719.37	3139.57	2514.33	1904.32
Ext 10	9220.11	3382.22	2687.83	2101.09

Fig. 9. DMA results: (a) storage modulus (E') and (b) damping factor (Tanδ) as a function of temperature for the reprocessed polymer blend.
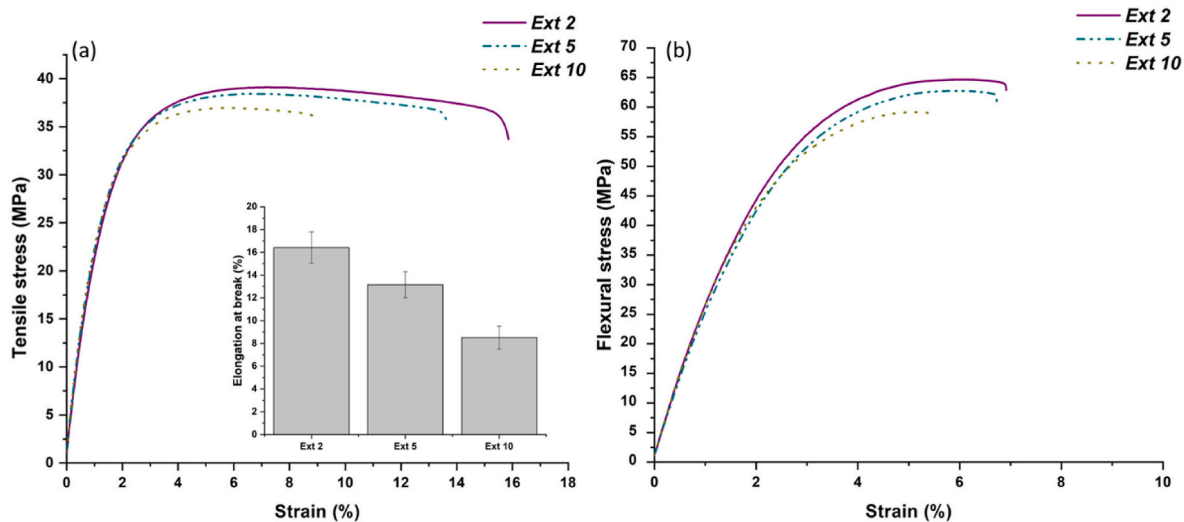
Fig. 10. Quasi-static tests of reprocessed polymer: (a) tensile and (b) three-point bending results.

Table 3
Mechanical properties of reprocessed blends.

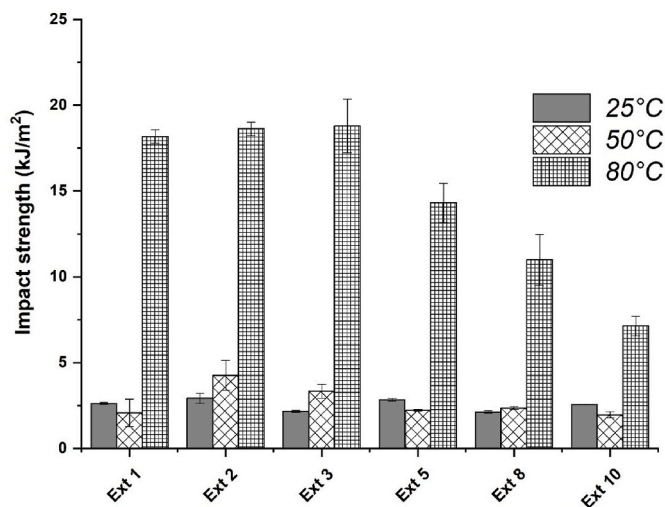| Sample	Tensile strength (MPa)	Young's modulus (GPa)	Flexural strength (MPa)	Flexural modulus (GPa)
Ext 1	38.4 ± 0.8	2.5 ± 0.1	63.4 ± 1.3	2.7 ± 0.1
Ext 2	38.9 ± 0.7	2.4 ± 0.1	64.9 ± 1.0	2.8 ± 0.1
Ext 3	38.6 ± 0.1	2.6 ± 0.1	62.9 ± 0.7	2.7 ± 0.1
Ext 5	38.4 ± 0.2	2.5 ± 0.1	62.3 ± 0.8	2.7 ± 0.1
Ext 8	36.8 ± 0.1	2.7 ± 0.1	59.8 ± 0.3	2.7 ± 0.1
Ext 10	36.9 ± 0.2	2.7 ± 0.1	59.3 ± 0.5	2.8 ± 0.1

Fig. 11. Charpy impact strength test results of reprocessed polymer.

reprocessing, a reduction in the crystallinity of the polymer blend was observed, showing approximately a 20 % decrease for PLA and an 11 % decrease for PBS. Moreover, multiple processing cycles led to thermal degradation, resulting in about a 33 % decrease for PLA and a 4 % decrease for PBS. In addition, the thermo-mechanical stresses contributed to molecular chain scission, as revealed by a decrease in the weight-average molecular weight (M_w) and an increase in the melt flow rate (MFR) of the material.

However, despite these observed changes, rheological analysis revealed the occurrence of crosslinking, indicated by an increase in complex viscosity at low frequencies. This balancing act between the reduction in crystallinity and thermal degradation, alongside the occurrence of crosslinking, contributed to maintaining good mechanical properties. There was an observed decrease in tensile and bending strength of approximately 3.8 % and 6.4 %, respectively, from the first to the tenth reprocessing cycle. However, the tensile and flexural moduli remained substantially unchanged. Overall, these results suggest the good attitude of the material towards recycling. This study represents an attempt to assess the effects of recycling a commercial biodegradable polymer blend, employing systems close to real industrial equipment but within a laboratory-scale dimension. It is crucial to note that the feed of the reprocessed material, as well as the forces and pressures involved in this process, are lower than those encountered in actual industrial settings. Therefore, it is necessary to highlight that the scale-up of the process needs additional investigations to support the findings presented here.

Funding

CRediT authorship contribution statement

Irene Bavasso: Writing – original draft, Methodology, Investigation, Formal analysis, Data curation. **Maria Paola Bracciale:** Formal analysis, Data curation, Investigation, Writing – original draft. **Giovanni De Bellis:** Data curation, Formal analysis, Investigation, Writing – original draft. **Alessia Pantaleoni:** Data curation, Formal analysis. **Jacopo Tirillò:** Methodology, Project administration, Resources, Supervision, Writing – review & editing. **Genny Pastore:** Data curation, Formal analysis, Writing – review & editing. **Serena Gabrielli:** Data curation, Formal analysis, Writing – review & editing. **Fabrizio Sarasini:** Conceptualization, Methodology, Supervision, Writing – review & editing.
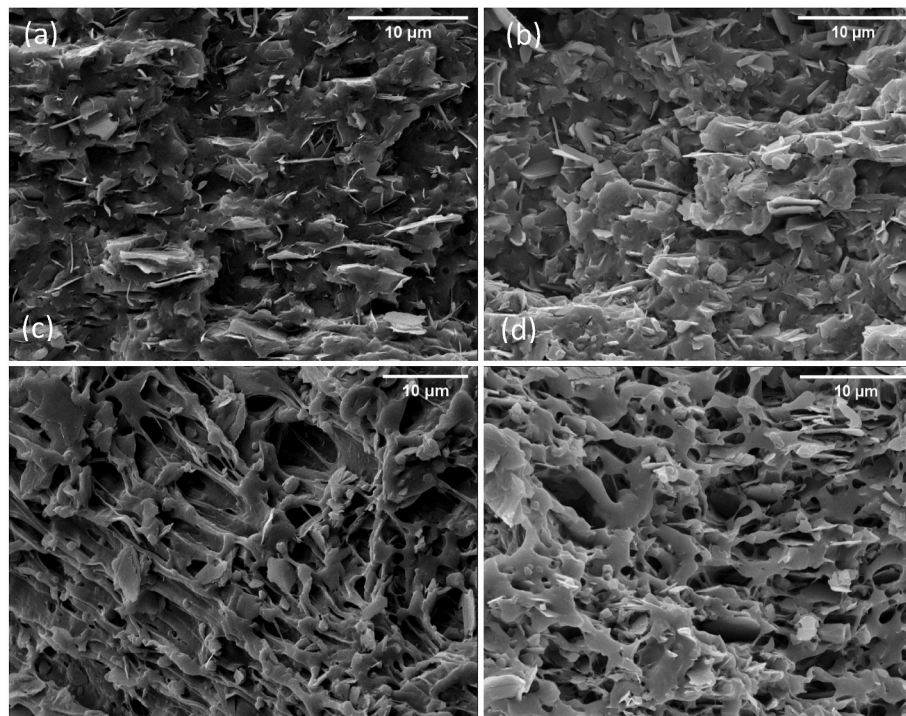
Fig. 12. SEM micrographs of the impact-fractured surfaces of reprocessed polymer after the first extrusion/injection cycle at (a) 25 °C and (c) 80 °C and after the tenth extrusion/injection cycle at (b) 25 °C and (d) 80 °C.

Declaration of competing interest

The authors declare that they have no known competing financial interests or personal relationships that could have appeared to influence the work reported in this paper.

Data availability

Data will be made available on request.

Appendix A. Supplementary data

Supplementary data to this article can be found online at https://doi.org/10.1016/j.polymertesting.2024.108418.

References

[1] C. Gioia, G. Giacobazzi, M. Vannini, G. Totaro, L. Sisti, M. Colonna, et al., End of life of biodegradable plastics: composting versus Re/upcycling, ChemSusChem 14 (2021) 4167–4175, https://doi.org/10.1002/cssc.202101226.

[2] T.P. Haider, C. Völker, J. Kramm, K. Landfester, F.R. Wurm, Plastics of the future? The impact of biodegradable polymers on the environment and on society, Angew. Chem. Int. Ed. 58 (2019) 50–62, https://doi.org/10.1002/anie.201805766.

[3] A. Soroudi, I. Jakubowicz, Recycling of bioplastics, their blends and biocomposites: a review, Eur. Polym. J. 49 (2013) 2839–2858, https://doi.org/10.1016/j.eurpolymj.2013.07.025.

[4] P. Rai, S. Mehrotra, S. Priya, E. Gnansounou, S.K. Sharma, Recent advances in the sustainable design and applications of biodegradable polymers, Bioresour. Technol. 325 (2021) 124739, https://doi.org/10.1016/j.biortech.2021.124739.

[5] M. Niaounakis, Recycling of biopolymers – the patent perspective, Eur. Polym. J. 114 (2019) 464–475, https://doi.org/10.1016/j.eurpolymj.2019.02.027.

[6] I. Dedieu, S. Peyron, N. Gontard, C. Aouf, The thermo-mechanical recyclability potential of biodegradable biopolyesters: perspectives and limits for food packaging application, Polym. Test. 111 (2022), https://doi.org/10.1016/j.polymertesting.2022.107620.

[7] M. Rajendran, M. Manjusri, M. Amar Kumar, Biodegradable Compatibilized Polymer Blends for Packaging Applications: A Literature Review, vol. 135, 2018, https://doi.org/10.1002/app.46279.

[8] I. Zembouai, S. Bruzaud, M. Kaci, A. Benhamida, Y.M. Corre, Y. Grohens, Mechanical recycling of poly(3-hydroxybutyrate-co-3-hydroxyvalerate)/polylactide based blends, J. Polym. Environ. 22 (2014) 449–459, https://doi.org/10.1007/s10924-014-0684-5.

[9] N.C. Farias, I. Major, D. Devine, M. Brennan Fournet, R. Pezzoli, Taghinezhad S. Farshbaf, et al., Multiple recycling of a PLA/PHB biopolymer blend for sustainable packaging applications: rheology-morphology, thermal, and mechanical performance analysis, Polym. Eng. Sci. 62 (2022) 1764–1774, https://doi.org/10.1002/pen.25962.

[10] A. Bourmaud, D. Åkesson, J. Beaugrand, A. Le Duigou, M. Skrifvars, C. Baley, Recycling of L-Poly-(lactide)-Poly-(butylene-succinate)-flax biocomposite, Polym. Degrad. Stabil. 128 (2016) 77–88, https://doi.org/10.1016/j.polymdegradstab.2016.03.018.

[11] M. Morreale, A. Liga, M.C. Mistretta, L. Ascione, F.P. La Mantia, Mechanical, thermomechanical and reprocessing behavior of green composites from biodegradable polymer and wood flour, Materials 8 (2015) 7536–7548, https://doi.org/10.3390/ma8115406.

[12] K. Resch-Fauster, A. Klein, E. Blees, M. Feuchter, Mechanical recyclability of technical biopolymers: potential and limits, Polym. Test. 64 (2017) 287–295, https://doi.org/10.1016/j.polymertesting.2017.10.017.

[13] Mantia FP. La, L. Botta, M.C. Mistretta, A Di Fiore, V. Titone, Recycling of a biodegradable polymer blend, Polymers 12 (2020) 1–12, https://doi.org/10.3390/polym12102297.

[14] M. Kervran, C. Vagner, M. Cochez, M. Ponçot, M.R. Saeb, H. Vahabi, Thermal degradation of polylactic acid (PLA)/polyhydroxybutyrate (PHB) blends: a systematic review, Polym. Degrad. Stabil. 201 (2022), https://doi.org/10.1016/j.polymdegradstab.2022.109995.

[15] S.F. Yao, X.T. Chen, H.M. Ye, Investigation of structure and crystallization behavior of poly(butylene succinate) by fourier Transform infrared spectroscopy, J. Phys. Chem. B 121 (2017) 9476–9485, https://doi.org/10.1021/acs.jpcb.7b07954.

[16] J.R. Riba, R. Cantero, V. García-Masabet, J. Cailloux, T. Canals, M.L. Maspoch, Multivariate identification of extruded PLA samples from the infrared spectrum, J. Mater. Sci. 55 (2020) 1269–1279, https://doi.org/10.1007/s10853-019-04091-6.

[17] X. Huang, J. Li, X. Su, K. Fang, Z. Wang, L. Liu, et al., Remarkable damage in talc caused by electron beam irradiation with a dose of up to 1000 kGy: lattice shrinkage in theZ- andY-axis and corresponding intrinsic microstructural transformation process speculation, RSC Adv. 11 (2021) 21870–21884, https://doi.org/10.1039/d1ra04012j.

[18] B. Pollakowski-Herrmann, A. Hornemann, A.M. Giovannozzi, F. Green, P. Gunning, C. Portesi, et al., A calibration procedure for a traceable contamination analysis on medical devices by combined X-ray spectrometry and ambient spectroscopic techniques, J. Pharm. Biomed. Anal. 150 (2018) 308–317, https://doi.org/10.1016/j.jpba.2017.12.007.

[19] R. Supthanyakul, N. Kaabbuathong, S. Chirachanchai, Poly(L-lactide-b-butylene succinate-b-L-lactide) triblock copolymer: a multi-functional additive for PLA/PBS blend with a key performance on film clarity, Polym. Degrad. Stabil. 142 (2017) 160–168, https://doi.org/10.1016/j.polymdegradstab.2017.05.029.

[20] J.B. Zeng, Y.D. Li, Q.Y. Zhu, K.K. Yang, X.L. Wang, Y.Z. Wang, A novel biodegradable multiblock poly(ester urethane) containing poly(l-lactic acid) and

poly(butylene succinate) blocks, Polymer 50 (2009) 1178–1186, https://doi.org/10.1016/j.polymer.2009.01.001.

[21] M. Oliveira, E. Santos, A. Araújo, G.J.M. Fechine, A.V. Machado, G. Botelho, The role of shear and stabilizer on PLA degradation, Polym. Test. 51 (2016) 109–116, https://doi.org/10.1016/j.polymertesting.2016.03.005.

[22] P.M. Chou, M. Mariatti, A. Zulkifli, M. Todo, Changes in the crystallinity and mechanical properties of poly(l-lactic acid)/poly(butylene succinate-co-l-lactate) blend with annealing process, Polym. Bull. 67 (2011) 815–830, https://doi.org/10.1007/s00289-011-0456-5.

[23] A. Anstey, S. Muniyasamy, M.M. Reddy, M. Misra, A. Mohanty, Processability and biodegradability evaluation of composites from poly(butylene succinate) (PBS) bioplastic and biofuel Co-products from ontario, J. Polym. Environ. 22 (2014) 209–218, https://doi.org/10.1007/s10924-013-0633-8.

[24] S.H. Ghaffar, O.A. Madyan, M. Fan, J. Corker, The influence of additives on the interfacial bonding mechanisms between natural fibre and biopolymer composites, Macromol. Res. 26 (2018) 851–863, https://doi.org/10.1007/s13233-018-6119-8.

[25] A. Shakoor, N.L. Thomas, Talc as a nucleating agent and reinforcing filler in poly (lactic acid) composites, Polym. Eng. Sci. 54 (2014) 64–70, https://doi.org/10.1002/pen.23543.

[26] K. Helanto, R. Talja, O.J. Rojas, Talc reinforcement of polylactide and biodegradable polyester blends via injection-molding and pilot-scale film extrusion, J. Appl. Polym. Sci. 138 (2021) 1–11, https://doi.org/10.1002/app.51225.

[27] M. Barletta, P. Moretti, E. Pizzi, M. Puopolo, V. Tagliaferri, S. Vesco, Engineering of Poly Lactic Acids (PLAs) for melt processing: material structure and thermal properties, J. Appl. Polym. Sci. 134 (2017) 1–12, https://doi.org/10.1002/app.44504.

[28] M.R. Nanda, M. Misra, A.K. Mohanty, The effects of process engineering on the performance of PLA and PHBV blends, Macromol. Mater. Eng. 296 (2011) 719–728, https://doi.org/10.1002/mame.201000417.

[29] A. Dmitruk, J. Ludwiczak, M. Skwarski, P. Makuła, P. Kaczyński, Influence of PBS, PBAT and TPS content on tensile and processing properties of PLA-based polymeric blends at different temperatures, J. Mater. Sci. 58 (2023) 1991–2004, https://doi.org/10.1007/s10853-022-08081-z.

[30] E.S. Yoo, S.S. Im, Melting behavior of poly(butylene succinate) during heating scan by DSC, J. Polym. Sci. B Polym. Phys. 37 (1999) 1357–1366, https://doi.org/10.1002/(SICI)1099-0488(19990701)37:13<1357::AID-POLB2>3.0.CO;2-Q.

[31] E. Quero, A.J. Müller, F. Signori, M.B. Coltelli, S. Bronco, Isothermal cold-crystallization of PLA/PBAT blends with and without the addition of acetyl tributyl citrate, Macromol. Chem. Phys. 213 (2012) 36–48, https://doi.org/10.1002/macp.201100437.

[32] T. Yokohara, M. Yamaguchi, Structure and properties for biomass-based polyester blends of PLA and PBS, Eur. Polym. J. 44 (2008) 677–685, https://doi.org/10.1016/j.eurpolymj.2008.01.008.

[33] X. Hu, T. Su, P. Li, Z. Wang, Blending modification of PBS/PLA and its enzymatic degradation, Polym. Bull. 75 (2018) 533–546, https://doi.org/10.1007/s00289-017-2054-7.

[34] V. Ojijo, S. Sinha Ray, R. Sadiku, Role of specific interfacial area in controlling properties of immiscible blends of biodegradable polylactide and poly[(butylene succinate)-co-adipate], ACS Appl. Mater. Interfaces 4 (2012) 6690–6701, https://doi.org/10.1021/am301842e.

[35] F.R. Beltrán, M.P. Arrieta, E. Moreno, G. Gaspar, L.M. Muneta, R. Carrasco-Gallego, et al., Evaluation of the technical viability of distributed mechanical recycling of PLA 3D printing wastes, Polymers 13 (2021), https://doi.org/10.3390/polym13081247.

[36] F.R. Beltrán, M.U. de la Orden, V. Lorenzo, E. Pérez, M.L. Cerrada, J. Martínez Urreaga, Water-induced structural changes in poly(lactic acid) and PLLA-clay nanocomposites, Polymer 107 (2016) 211–222, https://doi.org/10.1016/j.polymer.2016.11.031.

[37] A. Leroy, S. Ribeiro, C. Grossiord, A. Alves, R.H. Vestberg, V. Salles, et al., FTIR microscopy contribution for comprehension of degradation mechanisms in PLA-based implantable medical devices, J. Mater. Sci. Mater. Med. 28 (2017), https://doi.org/10.1007/s10856-017-5894-7.

[38] J. Zhang, Y. Duan, H. Sato, H. Tsuji, I. Noda, S. Yan, et al., Crystal modifications and thermal behavior of poly(L-lactic acid) revealed by infrared spectroscopy, Macromolecules 38 (2005) 8012–8021, https://doi.org/10.1021/ma051232r.

[39] L.-Q. Xu, H.-X. Huang, Relaxation behavior of poly(lactic acid)/Poly(butylene succinate) blend and a new method for calculating its interfacial tension, J. Appl. Polym. Sci. 125 (2012) E272–E277, https://doi.org/10.1002/app.

[40] F.L. Chang, B. Hu, W.T. Huang, L. Chen, X.C. Yin, X.W. Cao, et al., Improvement of rheology and mechanical properties of PLA/PBS blends by in-situ UV-induced reactive extrusion, Polymer 259 (2022), https://doi.org/10.1016/j.polymer.2022.125336.

[41] F. Casamento, A. D'Anna, R. Arrigo, A. Frache, Rheological behavior and morphology of poly(lactic acid)/low-density polyethylene blends based on virgin and recycled polymers: compatibilization with natural surfactants, J. Appl. Polym. Sci. 138 (2021), https://doi.org/10.1002/app.50590.

[42] H. Jin, J. Gonzalez-Gutierrez, P. Oblak, B. Zupančič, I. Emri, The effect of extensive mechanical recycling on the properties of low density polyethylene, Polym. Degrad. Stabil. 97 (2012) 2262–2272, https://doi.org/10.1016/j.polymdegradstab.2012.07.039.

[43] I.N. Georgousopoulou, S. Vouyiouka, P. Dole, C.D. Papaspyrides, Thermo-mechanical degradation and stabilization of poly(butylene succinate), Polym. Degrad. Stabil. 128 (2016) 182–192, https://doi.org/10.1016/j.polymdegradstab.2016.03.012.

[44] I. Pillin, N. Montrelay, A. Bourmaud, Y. Grohens, Effect of thermo-mechanical cycles on the physico-chemical properties of poly(lactic acid), Polym. Degrad. Stabil. 93 (2008) 321–328, https://doi.org/10.1016/j.polymdegradstab.2007.12.005.

[45] A. Le Duigou, I. Pillin, A. Bourmaud, P. Davies, C. Baley, Effect of recycling on mechanical behaviour of biocompostable flax/poly(l-lactide) composites, Composer Part A Appl Sci Manuf 39 (2008) 1471–1478, https://doi.org/10.1016/j.compositesa.2008.05.008.

[46] F. Carrasco, P. Pagès, J. Gámez-Pérez, O.O. Santana, M.L. Maspoch, Processing of poly(lactic acid): characterization of chemical structure, thermal stability and mechanical properties, Polym. Degrad. Stabil. 95 (2010) 116–125, https://doi.org/10.1016/J.POLYMDEGRADSTAB.2009.11.045.

[47] J.P. Lopez, J. Girones, J.A. Mendez, J. Puig, M.A. Pelach, Recycling ability of biodegradable matrices and their cellulose-reinforced composites in a plastic recycling stream, J. Polym. Environ. 20 (2012) 96–103, https://doi.org/10.1007/s10924-011-0333-1.

[48] R. Al-Itry, K. Lamnawar, A. Maazouz, Improvement of thermal stability, rheological and mechanical properties of PLA, PBAT and their blends by reactive extrusion with functionalized epoxy, Polym. Degrad. Stabil. 97 (2012) 1898–1914, https://doi.org/10.1016/j.polymdegradstab.2012.06.028.

[49] P. Srimalanon, I. Martín-Fabiani, B. Prapagdee, T. Markpin, E. Wimolmala, N. Sombatsompop, Influence of reprocessing cycles on mechanical and antibacterial performances of hygienic in situ compatibilized PBS/PLA blends doped with HPQM, J. Mater. Cycles Waste Manag. 23 (2021) 1893–1904, https://doi.org/10.1007/s10163-021-01259-8.

[50] N. Singh, B. Mann, R. Sharma, A. Verma, N.R. Panjagari, K. Gandhi, Identification of polymer additives from multilayer milk packaging materials by liquid-solid extraction coupled with GC-MS, Food Packag. Shelf Life 34 (2022), https://doi.org/10.1016/j.fpsl.2022.100975.

[51] L. Chen, Q. Dou, Influence of the combination of nucleating agent and plasticizer on the non-isothermal crystallization kinetics and activation energies of poly(lactic acid), J. Therm. Anal. Calorim. 139 (2020) 1069–1090, https://doi.org/10.1007/s10973-019-08507-y.

[52] T. Ramos-Hernández, J.R. Robledo-Ortíz, M.E. González-López, A.S.M. del Campo, R. González-Núñez, D. Rodrigue, et al., Mechanical recycling of PLA: effect of weathering, extrusion cycles, and chain extender, J. Appl. Polym. Sci. 140 (2023), https://doi.org/10.1002/app.53759.

[53] N. Dulal, R. Shanks, T. Gengenbach, H. Gill, D. Chalmers, B. Adhikari, et al., Slip-additive migration, surface morphology, and performance on injection moulded high-density polyethylene closures, J. Colloid Interface Sci. 505 (2017) 537–545, https://doi.org/10.1016/j.jcis.2017.06.040.

[54] J. Shojaeiarani, D.S. Bajwa, C. Rehovsky, S.G. Bajwa, G. Vahidi, Deterioration in the physico-mechanical and thermal properties of biopolymers due to reprocessing, Polymers 11 (2019) 58, https://doi.org/10.3390/polym11010058.

[55] A. Agüero, M. Morcillo, C. del, L. Quiles-Carrillo, R. Balart, T. Boronat, D. Lascano, et al., Study of the influence of the reprocessing cycles on the final properties of polylactide pieces obtained by injection molding, Polymers 11 (2019), https://doi.org/10.3390/polym11121908.

[56] G.C. Liu, W.Q. Zhang, S.L. Zhou, X.L. Wang, Y.Z. Wang, Improving crystallization and processability of PBS: via slight cross-linking, RSC Adv. 6 (2016) 68942–68951, https://doi.org/10.1039/c6ra13488b.

[57] P. Ma, D.G. Hristova-Bogaerds, P.J. Lemstra, Y. Zhang, S. Wang, Toughening of PHBV/PBS and PHB/PBS blends via in situ compatibilization using dicumyl peroxide as a free-radical grafting initiator, Macromol. Mater. Eng. 297 (2012) 402–410, https://doi.org/10.1002/mame.201100224.